

Massive MIMO Communication With Adaptive Interference Suppression Algorithm For Irregular Antenna Arrays

B.HemaPriyadharshini V.Bhuvaneshwari M.Kavitha R.Arasa Kumar
Department of Electronics and Communication Engineering,
Velammal College of Engineering & Technology, Madurai, TamilNadu, India.

Abstract - In practical mobile communication engineering applications, surfaces of antenna array exploitation sections are usually irregular. Hence massive MIMO wireless communication system broadcast the wireless data signal using irregular antenna arrays. To estimate the performance of irregular antenna array, the matrix correlation coefficient along with the ergodic received gain is defined for massive MIMO communication systems with common coupling effects. Statistical results indicate that there exists a highest achievable rate when the number of antennae keeps increasing in massive MIMO communication systems using irregular antenna arrays. An Adaptive interferences suppression method is proposed to configure the large antenna array by following a subarray configuration (SC). Furthermore, a robust adaptive decision-feedback (DF) GSC with the least-mean-square (LMS) algorithm has proposed to effectively suppress unwanted interference and ingress the maximum extent. Moreover, the irregular antenna array outperforms the regular antenna array in the attainable rate of massive MIMO communication systems when the number of antennae is better than or equal to a given threshold.

Index Terms— Massive MIMO, irregular antenna array, mutual coupling, achievable rate.

I. INTRODUCTION

The massive multi-input-multi-output (MIMO) technology is obtainable as one of the key technologies for the fifth generation (5G) wireless communication systems [1]–[3].

Massive MIMO systems be able to improve the spectrum efficiency to 10-20 bit/s/Hz level and accumulate 10-20 times energy within wireless communication systems [4]. nevertheless, considering a incomplete available physical space for deployment of large number of antenna elements in base stations (BSs), the mutual coupling effect among antenna elements is inevitable for massive MIMO wireless communication systems [5], [6]. Moreover, with hundreds of antennas arranged, new problems of the antenna array deployment and architecture may appear [7].

When antennas are intimately deployed in an antenna array, the communication between two or more antennas, i.e., the joint coupling effect, is predictable and affects coefficients of the antenna array [8]. The mutual

coupling effect has been widely studied in antenna propagation and signal processing topics [9], [10]. Based on the theoretical analysis and experimental measurement, the performance of antenna array was compared with or without the mutual coupling effect in [9]. It was shown that the mutual coupling significantly affects the performance of adaptive antenna arrays with either large or small inter-element spacing because the steering vector of the antenna array has to be modified both in phases and amplitudes [10]. With the MIMO technology emerging in wireless communication systems, the collision of mutual coupling on MIMO systems has been studied [11]–[14].

To further improve the transmission rate in 5G wireless communication systems, the massive MIMO technology is envisaged to satisfy 1000 times wireless traffic increase in the future decade [15]–[17]. Marzetta revealed that all effects of uncorrelated noise and fast fading will disappear when the number of antennas grows without limit in wireless communication systems [15]. Moreover, massive MIMO systems could improve the spectrum efficiency by one or two orders of magnitude and the energy efficiency by three orders of magnitude for wireless communication systems [16], [18]. New precoding and estimation schemes have also been investigated for massive MIMO systems [19], [20]. Motivated by these results, the impact of mutual coupling on massive MIMO systems was explored in recently literatures. For massive MIMO systems where dipole antennas are placed in a fixed length linear array, analytical results indicated that some ignoring effects, such as mutual coupling effect, give misleading results in wireless communication systems. Based on different antenna elements, such as dipole, patch and dualpolarized patch antennas, it was demonstrated that the mutual coupling and spatial correlation have practical limit on the spectrum efficiency of multi-user massive MIMO systems. Considering the spatial correlation and mutual coupling effects on massive MIMO systems, the performance of linear precoders was analyzed for wireless communications systems. However, in all aforementioned studies, only regular antenna arrays were considered for massive MIMO

systems with the mutual coupling effect. Considering the aesthetic appearance of the commercial buildings, building a platform with a large number of regular antennas on the facade will face confrontations from the building owners. To tackle the challenge of deploying large number of BS antennas, the antennas elements were integrated into the environments, such as a part of the building facade or signage [7]. Moreover, the large number of antennas make it very difficult to maintain uniform antenna spacings in these scenarios. As a consequence, these antenna arrays are appropriate to be considered as irregular antenna arrays with nonuniform antenna spacings rather than regular antenna arrays with uniform antenna spacings. For irregular antenna arrays, some studies have been made for conformal antenna arrays where antenna arrays are designed to confirm the prescribed shape. Sparse antenna arrays where antenna arrays are configured to decrease the number of antennas but lead to non-uniform antenna spacings and irregular array shapes have also been studied. However, these antenna arrays were mainly studied in the field of phased arrays and have never been discussed for massive MIMO communication systems. Motivated by the above gaps, we investigate multi-user massive MIMO wireless communication systems with irregular antenna arrays considering the mutual coupling. The contributions and novelties of this paper are summarized as follows

- 1) Considering uneven surfaces of antennas deployment regions, a massive MIMO communication system with an irregular antenna array is firstly proposed and formulated. Moreover, the impact of mutual coupling on irregular antenna arrays is evaluated by metrics of the matrix correlation coefficient and ergodic received gain.
- 2) Based on the results of irregular antenna arrays with mutual coupling, the lower bound of the ergodic achievable rate, average symbol error rate (SER) and average outage probability are derived for multi-user massive MIMO communication systems. Furthermore, asymptotic results are also derived when the number of antennas approaches infinity.
- 3) Numerical results indicate that there exists a maximum achievable rate for massive MIMO communication systems using irregular antenna arrays. Moreover, the irregular antenna array outperforms the regular antenna array in the achievable rate of massive MIMO communication systems when the number of antennas is larger than or equal to a given threshold.

The remainder of this paper is outlined as follows. Section II describes a system model for massive MIMO communication systems where BS antennas are deployed by an irregular antenna array. In Section III, the impact of mutual coupling on the irregular antenna array is analyzed by the matrix correlation coefficient and ergodic received

gain. In section IV, the lower bound of the ergodic achievable rate, average SER and average outage probability are derived for multi-user massive MIMO communication systems using irregular antenna arrays. Considering that the number of antennas approaches infinity, asymptotic results are also obtained. Numerical results and discussions are presented in Section V. Finally, conclusions are drawn in Section VI.

II. SYSTEM MODEL

Surfaces used for deploying the antennae are not ideally smooth in Real time. Spatial distances among adjacent antennas are not expected to be perfectly uniform when massive MIMO is used. So massive MIMO communication systems have been deployed. So the impact of irregular antenna arrays on massive MIMO communication systems need to be reevaluated when the mutual coupling of irregular antenna arrays is taken for consideration. BS is located at the cell center with M antennas deployed on unequal surface.

In this system model, a BS is located at the cell center and equipped with M antennas which are deployed on an uneven surface. A spatial distance among antennas is no longer regular even when antennas are regularly deployed in a two-dimensional plane.

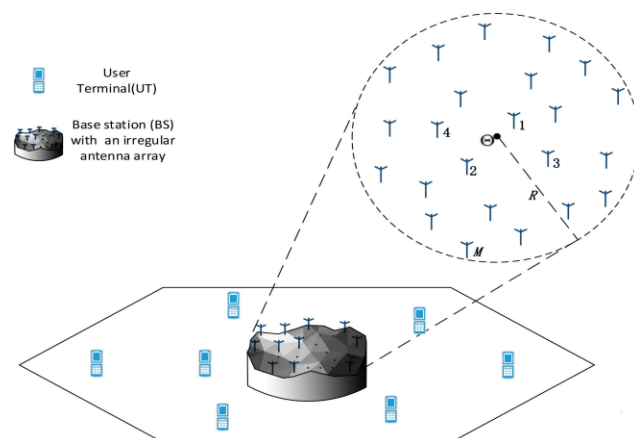


Fig.1. Multi-user massive MIMO communication system with irregular antenna array.

In the projected plane of Fig. 1, without loss of generality, all antennas are assumed to be covered by a circle centered at Θ with the radius R . The i -th and j -th antennas of the massive MIMO antenna array are denoted as Ant_i and Ant_j ; $i \neq j$, $1 \leq i \leq M$, $1 \leq j \leq M$. Spatial distances between the circle center Θ and locations of the antennas Ant_i and Ant_j are denoted as d_i and d_j , respectively. And i.e., $d_i < d_j$ if $i < j$. The distribution of the M antennas in the circle is assumed to be governed by a binomial point process (BPP). It's notable that the circle area is an assumed area on the smooth projection plane to cover all antennas. The circle area does not depend on the

actual shape of the antenna deployment regions. Similarly, other random processes can be used for modeling of the irregular antenna distribution according to the specified requirements. K active user terminals (UTs) are assumed to be uniformly scattered in a cell and each UT is equipped with an antenna. In this paper, we focus on the uplink transmission of the massive MIMO communication system.

The signal vector received at the BS is expressed as

$$y = \sqrt{SNR_{UT}}GX + w$$

Where $y \in \mathbb{C}^{M \times 1}$ is the $M \times 1$ received signal vector, $w \in \mathbb{C}^{M \times 1}$ is the additive white Gaussian noise(AWGN) with zero mean, $w \sim \mathcal{CN}(0, I_M)$, I_M is the $M \times M$ unit matrix, $x \in \mathbb{C}^{K \times 1}$ is the $K + 1$ symbol vector transmitted by KUT_S . Moreover, the UT transmitting power is normalized as 1. SNR_{UT} is the transmitting signal-to-noise ratio (SNR) at the UT and values of SNR_{UT} at all UTs are assumed to be equal in this paper.

Similar to the finite dimensional physical channel and taking into account the mutual coupling effect between antennas, the $M \times K$ channel matrix $G \in \mathbb{C}^{M \times K}$ is extended as

$$G = CAHD^{1/2}$$

Where C is a mutual coupling matrix, A is an array steering matrix, H is a small scale fading matrix, and D is the large scale fading matrix. The mutual coupling matrix C and the array steering matrix A are affected by the irregularity of the antenna array. The detailed modeling of these two matrixes will be discussed in the next section. The large scale fading matrix is a $K \times K$ diagonal matrix and is expressed as

$$D = \text{diag}(\beta_1, \dots, \beta_k, \dots, \beta_K) \quad (3)$$

the k -th diagonal element of matrix D , i.e., β_k , denotes the large scale fading factor in the link of the k -th UT and the BS.. The propagation environment offers rich scattering if the number of independent incident directions is large in the angular domain. More precisely, a finitedimensional channel model is introduced in this paper, where the angular domain is divided into P independent incident directions with P being a large but finite number. Each independent incident direction, corresponding to the azimuth angle $\phi_q, \phi_q \in [0, 2\pi]$, $q = 1, \dots, P$ and the elevation angle $\theta_q, \theta_q \in [-\pi/2, \pi/2]$ is associated with an $M \times 1$ array steering vector $a_{\phi_q, \theta_q} \in \mathbb{C}^{M \times 1}$. In this case, all independent incident directions are associated with an $M \times P$ array steering matrix A which is given by expression (4)

$$A = [a(\phi_1, \theta_1), \dots, a(\phi_q, \theta_q), \dots, a(\phi_p, \theta_p)] \in \mathbb{C}^{M \times P} \quad (4)$$

Therefore, despite locations of UTs, the uplink signals are scattered by the scatters around the BS and arrive at the BS from the P incident directions. $H \in \mathbb{C}^{P \times K}$ is the $P \times K$ small scale fading matrix and extended as

$$H = [h_1, \dots, h_k, \dots, h_K] \in \mathbb{C}^{P \times K}, \quad (5a)$$

$$h_k = [h_{k,1}, \dots, h_{k,q}, \dots, h_{k,p}]^T, \quad (5b)$$

Where $h_{k,q}$ is the small scale fading factor in the link of the k -th UT and the BS at the q -th independent incident direction, which is governed by a complex Gaussian distribution with zero mean and unit variance, i.e., $h_{k,q} \sim \mathcal{CN}(0, 1)$. $C \in \mathbb{C}^{M \times M}$ is an $M \times M$ mutual coupling matrix which represents the mutual coupling effect on the irregular antenna array. More specifically, $[C]_{i,j} \neq 0$, i.e., the element at the i -th row and j -th column of C denotes the mutual coupling coefficient between the antennas Ant_i and Ant_j in the irregular antenna array.

III. IRREGULAR ANTENNA ARRAY WITH MUTUAL COUPLING

A. Channel Correlation Model

Since each UT is equipped with an antenna and UTs are assumed to be distributed far away from each other, channels of different UTs are assumed to be uncorrelated. In this section, the channel correlation is focused on the side of BS irregular antenna arrays. Based on the channel matrix G in (2), the channel correlation matrix is expressed by

$$\Psi = \frac{1}{K} D^{-1} E_H(GG^H) = CAA^H, \quad (6)$$

where D^{-1} is a normalizing result for the large scale fading, $E_H(\cdot)$ is an expectation operator taken over the small scale fading matrix H and the superscript H denotes the conjugate transpose of a matrix. Considering that the distribution of spatial distances among M antennas follows a binomial point process for irregular antenna arrays, the probability density function (PDF) of d_i is expressed as expression (7)

$$f_{d_i}(d) = \frac{2\Gamma(M+1)(R^2+d^2)^{M-i}d^{2i-1}}{R^{2M}\Gamma(i)\Gamma(M-i+1)} \quad (7)$$

$$d_{ij} = \sqrt{d_i^2 + d_j^2 - 2d_i d_j \cos\psi_{ij}}, \quad (8)$$

Z_{ij}

$$= \frac{\zeta}{4\pi} \begin{bmatrix} 2\left(\gamma + \ln(\zeta) + \int_0^\zeta \frac{\cos x - 1}{x} dx\right) \\ -\left(\gamma + \ln(\mu) + \int_0^\mu \frac{\cos x - 1}{x} dx\right) \\ -\left(\gamma + \ln(\rho) + \int_0^\rho \frac{\cos x - 1}{x} dx\right) \\ -j\left(2\int_0^\zeta \frac{\sin x}{x} dx - \int_0^\mu \frac{\sin x}{x} dx\right) \\ -\int_0^\rho \frac{\sin x}{x} dx \end{bmatrix}, \quad (9)$$

Where ζ is an impedance of free space, γ is an Euler-Mascheroni constant, l is an antenna length. Based on the

mutual impedance matrix \mathbf{ZC} , the mutual coupling matrix \mathbf{C} is expressed as [13]

$$\mathbf{C} = (\mathbf{Z}_0 + \mathbf{Z}_L) (\mathbf{Z}_L \mathbf{I}_M + \mathbf{Z}_C)^{-1} \quad (10)$$

Where \mathbf{Z}_L is the load impedance of each antenna. Considering the incident signal with azimuth angle ϕ_q and elevation angle θ_q , the phase response of the point with the coordinate

$$(d_x, \psi_x) \text{ is } \exp\left(-\frac{2\pi d_x}{\lambda} \alpha\right) \text{ in which } \alpha = \cos\psi_x \cos\phi_q \cos\theta_q + \sin\psi_x \sin\phi_q \sin\theta_q.$$

Therefore, the phase response of Ant_M with the coordinate $(d_M, 0)$ is given by

$$a_M(\phi_q, \theta_q) = \exp\left(-j \frac{2\pi d_M}{\lambda} \sin\theta_q \cos\phi_q\right) \quad (11)$$

For Ant_i with the spatial distance d_i in the projected plane of the corresponding position in the polar coordinate system is denoted as (d_i, ψ_i) . Similarly, given the polar coordinate of Ant_i , its phase response with the origin Θ as the phase response reference is derived by expression (12)

$$= \exp\left[-j \frac{2\pi d_i}{\lambda} \sin\theta_q \cos(\theta_q - \psi_i)\right]. \quad (12)$$

$$\eta = \frac{T_r[\Psi\Psi^H]}{T_r[\Psi^0\Psi]} - 1 \quad (13)$$

B. Ergodic Received Gain

To easily investigate the impact of the varying number of antennas and antenna spatial distance to the received SNR, the ergodic received gain of irregular antenna arrays is defined as

$$G(M, R) = E(SNR_{BS} - SNR_{BS}^{min}), \quad (14)$$

$$\tilde{y}_{1,MRC} = \sqrt{SNR_{UT}} \beta_1 h_1^H A^H C^H C A h_{1x} + \beta_1^{1/2} h_1^H A^H C^H \omega_1, \quad (15)$$

Where x is the symbol transmitted by the UT, ω_1 is the AWGN with zero mean over wireless channels. SNR_{UT} is the transmit SNR at the UT and equals to the transmit power of the UT. Furthermore, the received SNR at BS is given by

$$SNR_{1,BS,MRC} = SNR_{UT} \beta_1 h_1^H A^H C^H C A h_1 \quad (16)$$

For the single UT scenario, the minimum received SNR with the BS irregular antenna array, which is denoted as

$$SNR_{min,BS,MRC} \text{ is expressed by } SNR_{1,BS,MRC}^{min} = SNR_{UT} \beta_1 h_1^H \hat{A}^H \hat{C}^H \quad (17)$$

Where $\hat{\mathbf{C}}$ and $\hat{\mathbf{A}}$ are the mutual coupling matrix and array steering matrix with the minimum number of antennas M_{min} and the minimum circle radius R_{min} , respectively. Based on the definition of ergodic received gain in (14), the ergodic received gain with the single UT is derived by

$$G(M, R) = E(SNR_{1,BS,MRC} - SNR_{1,BS,MRC}^{min}) \quad (18)$$

Proposition 1: For the single UT scenario, the BS has the perfect channel state information and adopts the MRC detector scheme, the ergodic received gain at massive MIMO communication systems with irregular antenna arrays is derived by expression (19a)

$$G(M, R) = SNR_{UT} \beta_1 \frac{\det(B_M, 1)}{\prod_{i < j}^M (\tau_j - \tau_i)} \times \left[\left(\tau_M^M - \sum_{M-1}^{M-1} \sum_{M-1}^{M-1} [B_{M,1}^{-1}]_{q,p} \tau_M^{q-1} \tau_p^M \right) - \frac{\det(\hat{B}_{M_{min},1}, 1)}{\prod_{i < j}^{M_{min}} (\tau_j - \tau_i)} \left(\hat{\tau}_{M_{min}}^{M_{min}} - \sum_{p=1}^{M_{min}-1} \sum_{q=1}^{M_{min}-1} \times [\hat{B}_{M_{min},1}^{-1}]_{q,p} \hat{\tau}_{M_{min}}^{q-1} \hat{\tau}_p^{M_{min}} \right) \right], \quad (19a)$$

$$B_{M_{min},1} = \begin{bmatrix} 1 & \hat{\tau}_1 & \dots & \hat{\tau}_1^{M_{min}-2} \\ \vdots & \vdots & \ddots & \vdots \\ 1 & \hat{\tau}_{M_{min}-1} & \dots & \hat{\tau}_{M_{min}-1}^{M_{min}-2} \end{bmatrix}, \quad (19b)$$

Where $\hat{\tau}_p, 1 \leq p \leq M_{min}$ is the eigenvalue of channel correlation matrix $\hat{\mathbf{C}} \hat{\mathbf{A}} \hat{\mathbf{A}}^H \hat{\mathbf{C}}^H$. *Proof:* Based on the BS configuration and the single UT scenario, the ergodic received gain is expressed in (18a), (18b) and (18c). When all Eigen values $\tau_p, 1 \leq p \leq M$, of channel correlation matrix $\Psi = C A A^H C^H$ are assumed to be known, the conditional PDF of ξ_1 is derived by expression (20)

$$f_{\xi_1}(x | \tau_1, \dots, \tau_M) = \frac{\det(B_M, 1)}{\prod_{i < j}^M (\tau_j - \tau_i)} \times \left(\tau_M^{M-2} e^{-x/\tau_M} - \sum_{p=1}^{M-1} \sum_{q=1}^{M-1} [B_{M,1}^{-1}]_{q,p} \tau_M^{q-1} \tau_p^{M-2} e^{-x/\tau_p} \right), \quad (20)$$

Furthermore, the term of $E_{h_1}(\zeta_1)$ is derived by expression

$$\begin{aligned}
 &= \frac{\det(B_M, 1)}{\prod_{i < j}^M (\tau_j - \tau_i)} \left(\tau_M^{M-2} \int_0^{+\infty} x e^{-x/\tau_M} dx \right. \\
 &- \sum_{p=1}^{M-1} \sum_{q=1}^{M-1} [B_{M,1}^{-1}]_{q,p} \tau_M^{q-1} \tau_p^{M-2} \int_0^{+\infty} x e^{-x/\tau_M} dx \left. \right) \\
 &= \frac{\det(B_M, 1)}{\sum_{i < j}^M (\tau_j - \tau_i)} (\tau_M^M - (\sum_{p=1}^{M-1} \sum_{q=1}^{M-1} [B_{M,1}^{-1}]_{q,p} \tau_M^{q-1} \tau_p^M)) \\
 &= \frac{\det(B_M, 1)}{\sum_{i < j}^M (\tau_j - \tau_i)} \left(\tau_M^M \right. \\
 &\quad \left. - \left(\sum_{p=1}^{M-1} \sum_{q=1}^{M-1} [B_{M,1}^{-1}]_{q,p} \tau_M^{q-1} \tau_p^M \right) \right), \quad 21
 \end{aligned}$$

Similarly, the term of $E_{h_1}(\xi_{min})$ is derived by expression

$$\begin{aligned}
 &E_{h_1}(\xi_{min}) \\
 &= \frac{\det(\hat{B}_{M_{min},1})}{\sum_{i < j}^{M_{min}} (\tau_j - \tau_i)} \\
 &\times \left(\hat{\tau}_{M_{min}}^{M_{min}} \right. \\
 &- \sum_{p=1}^{M_{min}-1} \sum_{q=1}^{M_{min}-1} [\hat{B}_{M_{min},1}^{-1}]_{q,p} \hat{\tau}_{M_{min}}^{q-1} \hat{\tau}_p^{M_{min}} \left. \right), \quad (22)
 \end{aligned}$$

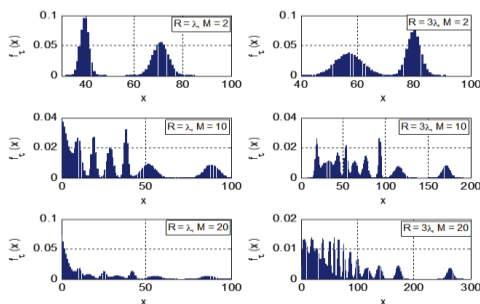


Fig.2. Empirical probability distribution of the eigenvalues of the channel correlation matrix Ψ .

C. Numerical Analysis

In the following analysis, default parameters in Fig. 1 are configured: antennas are assumed to be dipole antennas, the load impedance of every antenna is $Z_L = 50$ Ohms, the self-impedance of every antenna is 50 Ohms, the carry frequency used for wireless communications is 2.5 GHz, is $\lambda = 0.12$ meter (m), the number of independent incident directions in propagation environments is configured as $p = 100$. When the circle radius R is configured as λ and 3λ , Fig. 2 shows the empirical

distribution of the eigenvalues of the channel correlation matrix Ψ with the number of antennas $M=2, M=10, M=20$, respectively.

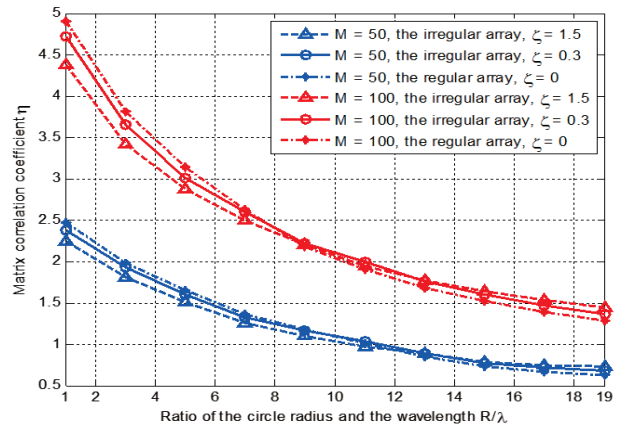


Fig3. Matrix correlation coefficient with respect to the ratio of the circle radius R and the wavelength λ , the number of antennas M and the irregularity coefficient ζ .

In Fig. 3, the matrix correlation coefficient with respect to the ratio of the circle radius and the wavelength, the number of antennas, and the irregularity coefficient are illustrated. It can be seen in Fig. 3 that the matrix correlation coefficient decreases with the increase of the ratio of the circle radius and the wavelength when the number of antennas and the irregular coefficient of the antenna array are fixed. When the array size is less than the cross point, the expectation of the average antenna spacing in the irregular

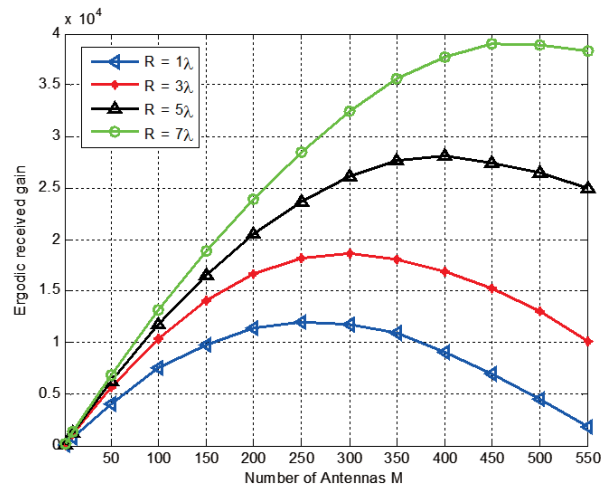


Fig4. Ergodic received gain with respect to the number of antennas and the circle radius.

array is larger than the average antenna spacing in the regular array. But when the array size is larger than the cross point, the expectation of the average antenna spacing in the irregular array is less than that in the regular array. Because the smaller average antenna spacing corresponds to the higher antenna correlation, the curves of regular

antenna arrays and irregular antenna arrays cross each other when the array size increases a given threshold. The impact of the number of antennas and the circle radius on the ergodic received gain of irregular antenna arrays with $\zeta = 1.5$ has been investigated in Fig. 4.

IV. MULTI-USER MASSIVE MIMO COMMUNICATION SYSTEMS

Based on the ergodic received gain of irregular antenna arrays, the lower bound of the ergodic achievable rate, the average SER and the average outage probability are presented for multi-user massive MIMO communication systems with irregular antenna arrays in this section. Then, the case with an infinite number of BS antennas is considered and asymptotic results are obtained for massive MIMO system performance metrics.

A. Achievable Rate

Assume that the zero-forcing detector is adopted at the BS to cancel the inter-user interference in the cell in Fig. 1. The BS detecting matrix is denoted as $F = G(G^H G)^{-1} \in \mathbb{C}^{M \times K}$. Therefore, the received signal at the BS is expressed as

$$\tilde{y} = \sqrt{SNR_{UT}} \times +F^H w \quad (23)$$

Considering the BS received signals transmitted from K active UTs, $\tilde{y} = [\tilde{y}_1, \dots, \tilde{y}_k, \dots, \tilde{y}_K] \in \mathbb{C}^{K \times 1}$ vector. The BS received signal transmitted from the k -th UT is expressed as

$$\tilde{y}_k = \sqrt{SNR_{UT}} x_k + F_k^H \quad (24)$$

Furthermore, the BS received SNR over the link of the k -th UT is expressed by

$$SNR_{k,BS,ZF} = \frac{SNR_{UT}}{\|F_k^H\|^2} = \frac{SNR_{UT}}{[(G^H G)^{-1}]_{kk}} \quad (25)$$

As a consequence, the achievable rate for the k -th UT is derived by expression (26)

$$E = \left[\log_2 \left\{ 1 + \frac{SNR_{UT}}{[(G^H G)^{-1}]_{kk}} \right\} \right] \quad (26)$$

Based on the channel matrix in (2), the closed-form solution of the lower bound of the ergodic achievable rate for the k -th UT is obtained in **Proposition 2**.

Proposition 2: For a single-cell multi-user massive MIMO communication system with BS irregular antenna arrays and the zero-forcing detector scheme, the closed-form expression of the lower bound of the uplink ergodic achievable rate for the k -th UT is given by expression (27a)

$$\begin{aligned} \check{R}_{k,ZF} = & \log_2 \left\{ 1 + SNR_{UT} \beta_k / \left[Y \sum_{i=1}^K \sum_{j=2}^K \Gamma(i-j) \right] \right\} \\ & \times D(i,j) \left(\tau_{n+i}^{n+j-2} - \sum_{p=1}^n \sum_{q=1}^n [B_{M,K}^{-1}]_{q,p} \tau_{n+i}^{q-1} \tau_p^{n+j-2} \right) \\ & + Y \sum_{i=1}^K D(i,j) \left(\tau_{n+i}^{n-1} - (\ln(\tau_{n+i}) - \gamma) \right. \\ & \left. - \sum_{p=1}^n \sum_{q=1}^n [B_{M,K}^{-1}]_{q,p} \tau_{n+i}^{q-1} \tau_p^{n-1} (\ln(\tau_p) \right. \\ & \left. - \gamma) \right) \Bigg\} \quad (27a) \end{aligned}$$

$$Y = \frac{\det(B_{M,K})}{K \prod_{q < p}^M (\tau_p - \tau_q) \prod_{p=1}^{K-1} p!} \quad (27b)$$

$$B_{M,K} = \begin{bmatrix} 1 & \tau_1 & \dots & \tau_1^{n-1} \\ \vdots & \vdots & \ddots & \vdots \\ 1 & \tau_n & \dots & \tau_n^{n-1} \end{bmatrix} \quad (27c)$$

When $n = M - K$, γ is the Euler-Mascheroni constant, $D(i, j)$ is the cofactor of the element $[\Omega]_{i,j}$ in the $K \times K$ matrix Ω , and the element $[\Omega]_{i,j}$ is expressed by expression (27d)

$$\begin{aligned} [\Omega]_{i,j} & = (j-1)! \tau_{n+i}^{n+j-1} \sum_{p=1}^n \sum_{q=1}^n [B_{M,K}^{-1}]_{p,q} \tau_{n+i}^{p-1} \tau_q^{n+j-1} \quad (27d) \end{aligned}$$

Proof: Substituting (2) into (26) and assuming that eigenvalues of the channel correlation matrix are known, the achievable rate for the k -th UT is derived by expression (28).

$$R_{k,ZF} = \log_2 \left\{ 1 + \frac{SNR_{UT} K \beta_k}{E(\sum_{i=1}^K \xi_i^{-1})} \right\} \quad (28)$$

Where $\xi_1, 1 \leq i \leq K$, is the i -th ordered eigenvalue of matrix $H^H A^H C^H C A H$. Let $f_\xi(x|\tau_1, \dots, \tau_M)$ denote the conditional marginal PDF of the unordered eigenvalues of matrix $H^H A^H C^H C A H$, and based on results in $f_\xi(x|\tau_1, \dots, \tau_M)$ is expressed by expression (29)

$$\begin{aligned} f_\xi(x|\tau_1, \dots, \tau_M) & = Y \sum_{i=1}^K \sum_{j=1}^K x^{j-1} D(i,j) \\ & \times \left(\tau_{n+i}^{n-1} e^{-x/\tau_{n+i}} - \sum_{p=1}^n \sum_{q=1}^n [B_{M,K}^{-1}]_{q,p} \tau_{n+i}^{q-1} \tau_{n+i}^{n-1} e^{-x/\tau_p} \right) \quad (29) \end{aligned}$$

Therefore, the term $\mathbb{E}(\sum_{i=1}^K \xi_i^{-1})$ in (28) is derived by expression (30)

$$\begin{aligned} & \mathbb{E}\left(\sum_{i=1}^K \xi_i^{-1}\right) \\ &= YK \left\{ \sum_{i=1}^K \sum_{j=2}^K \Gamma(j-1) D(i,j) \right. \\ & \times \left[\tau_{n+i}^{n+j-2} - \sum_{p=1}^n \sum_{q=1}^n [B_{M,K}^{-1}]_{q,p} \tau_{n+i}^{q-1} \tau_p^{n+j-2} \right] \\ & + \sum_{i=1}^K D(i,j) [\tau_{n+i}^{n-1} (\ln(\tau_{n+i}) - \gamma)] \\ & \left. - \sum_{p=1}^n \sum_{q=1}^n [B_{M,K}^{-1}]_{q,p} \tau_{n+i}^{q-1} \tau_p^{n-1} (\ln(\tau_p) - \gamma) \right\} \quad (30) \end{aligned}$$

Sub

$$\begin{aligned} R_{k,ZF} &\geq \left\{ \log_2 \left\{ 1 + \text{SNR}_{UT} \beta_k / \left[Y \sum_{i=1}^K \sum_{j=2}^K \Gamma(j-1) \times D(i,j) \right. \right. \right. \\ & \times \left. \left. \left(\tau_{n+i}^{n+j-2} - \sum_{p=1}^n \sum_{q=1}^n [B_{M,K}^{-1}]_{q,p} \tau_{n+i}^{q-1} \tau_p^{n+j-2} \right) \right. \right. \\ & \left. \left. + Y \sum_{i=1}^K D(i,j) (\tau_{n+i}^{n-1} (\ln(\tau_{n+i}) - \gamma)) \right. \right. \\ & \left. \left. - \sum_{p=1}^n \sum_{q=1}^n [B_{M,K}^{-1}]_{q,p} \tau_{n+i}^{q-1} \tau_p^{n-1} (\ln(\tau_p) - \gamma) \right\} \right\} \quad (31) \end{aligned}$$

and the lower bound of the ergodic achievable rate of the k th UT is just at the right side of the sign of inequality. Hence, **Proposition 2** gets proved. When all UTs are considered in the cell, the lower bound of the uplink ergodic achievable sum rate is derived by $R_{BS} = \sum_{k=1}^K R_{k,ZF}$. From

Proposition 2, In the following numerical results will be provided to illustrate the variation trend of the lower bound of the ergodic achievable rate with the changing of these parameters.

B. Symbol Error Rate

$$SER_{ZF} = \frac{1}{k} \sum_{k=1}^k \mathbb{E} \left[w_k Q \left(\sqrt{2 \bar{\omega}_k \text{SNR}_{k,BS,ZF}} \right) \right] \quad (32)$$

Where $Q(\cdot)$ is the Gaussian Q function while ω_k and $\bar{\omega}_k$ are modulation-specific constants. For the quadrature phase shift keying (QPSK) modulation, modulation-specific constants are configured as $\omega_k = 2$ and $\bar{\omega}_k = 0.5$. Assuming that all eigenvalues of channel correlation matrix $\Psi = CAA^H C^H$ are known.

C. Outage Probability

The outage probability is one of the most important metrics for wireless communication systems. Assuming the SNR

threshold is given by SNR_{th} , the average outage probability of multi-user massive MIMO communication systems with irregular antenna arrays is defined as [47]

$$P_{out} = \frac{1}{k} \sum_{k=1}^K P_r(\text{SNR}_{k,BS,ZF} \leq \text{SNR}_{th}) \quad (33)$$

Proposition 3: For a single-cell multi-user massive MIMO communication system with BS irregular antenna arrays and the zero-forcing detector scheme, the average outage probability of multi-user massive MIMO communication systems with is given by expression (34)

$$\begin{aligned} P_{out} &= \frac{1}{k} \sum_{k=1}^K Y \sum_{i=1}^K \sum_{j=1}^K D(i,j) \\ & \times \left(- \sum_{p=1}^n \sum_{q=1}^n [B_{M,k}^{-1}]_{q,p} \tau_{n+i}^{q-1} \vartheta(\tau_p, j) \right) \quad (34a) \\ \vartheta(x, y, k) &= (y-1)! x^{n+y-1} - \exp\left(-\frac{\text{SNR}_{th}}{\text{SNR}_{UT} \beta_k x}\right) \\ & \times \sum_{s=0}^{y-1} \frac{(y-1)!}{s!} \left(\frac{\text{SNR}_{th}}{\text{SNR}_{UT} \beta_k}\right)^s x^{n+y-s-3} \quad (34b) \end{aligned}$$

V. SIMULATION RESULTS AND DISCUSSIONS

Based on the proposed models of massive MIMO communicationsystems, the effect of mutual coupling on themassive MIMO communication systems with irregular andregular antenna arrays is analyzed by numerical simulations.In the following, some default parameters and assumptions arespecified. The type of all antennas at the BS is assumed to be the same, and the load impedance and self-impedance of eachantenna are assumed to be 50 Ohms [23]. The number of UTsin a cell is $K = 10$ and the large scale fading factor β_k ismodeled as $\beta_k = z / (l_k / l_{resist})^v$, which is similar to β_1 exceptwith l_k being a uniformly distributed random variable rangingfrom 10 m to 150 m [34], [35]. The transmitting SNR at eachUT is assumed to be 15 dB. Since the BS is assumed to be associated with a large but finite number of independentincident directions, the number of incident directions P areassumed to be 100. Fig. 5 illustrates the uplink ergodic achievable sum ratewith respect to the number of antennas M , the circle radius R and the irregularity coefficient ζ of antenna arrays. The linescorrespond to the lower bound of the uplink ergodic achievable sum rate \bar{R}_{BS} . The square points correspond to the asymptoticresults of the achievable sum rate obtained in (45). When thecircle radius is fixed, numerical results demonstrate that thereexists a maximum of the uplink ergodic achievable sum ratewith the increasing number of antennas. The uplinkErgodic

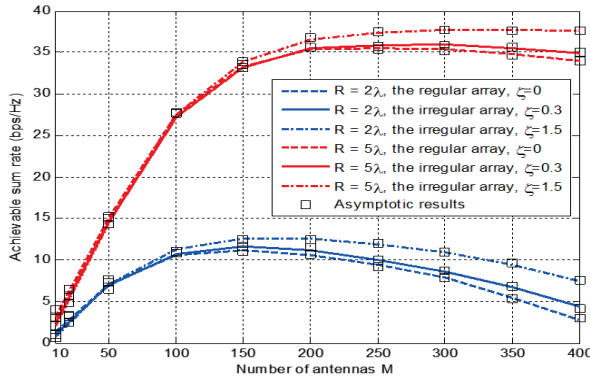


Fig5. The achievable sum rate with respect to the number of antennas, the circle radius and the irregularity coefficient.

sum rate increases with the increase of the number of antennas before achieving the maximum. After the number of antennas exceeds a given threshold, the uplink ergodic achievable sum rate becomes to decrease. When the number of antennas is fixed, the uplink ergodic achievable sum rate increases with the increase of the circle radius. Furthermore, it can be seen that the smaller value of the irregularity coefficient corresponds to the larger value of the achievable sum rate when the number of antennas is less than a given threshold. But when the number of antennas increases, curves with different irregularity coefficients get crossed. When the number of antennas is larger than a given threshold, the smaller value of the irregularity coefficient corresponds to the smaller value of the achievable sum rate. These results indicate that the irregular antenna array has contributed to improve the uplink ergodic achievable sum rate when the number of antennas is larger than or equal to a given threshold. In addition, the asymptotic results well match the lower bound of the uplink ergodic achievable sum rate in Fig. 5, especially when the number of antennas is large. Impact of the UT SNR and the number of BS antennas on the lower bound of the uplink ergodic achievable sum rate of multi-user massive MIMO communication systems with and without mutual coupling is investigated in Fig. 6. When the number of antennas at the BS is fixed, the lower bound of the uplink ergodic achievable sum rate increases with the increase of the UT SNR. When the UT SNR is fixed, the lower bound of the uplink ergodic achievable sum rate increases with the increase of the number of BS antennas. Moreover, the results of 10000 times Monte-Carlo simulation on the uplink ergodic achievable sum rate are illustrated. Both numerical and Monte-Carlo simulation results demonstrate that the uplink ergodic achievable sum rate with mutual coupling is less than the uplink ergodic achievable sum rate without mutual coupling for multi-user massive MIMO communication systems with irregular antenna arrays. Without loss of generality, the QPSK modulation scheme is adopted for numerical simulations in

Fig. 7. The modulation constants are configured as $\omega k = 2$ and $_k = 0.5$. Impact of the UT SNR, the number of BS antennas M and the circle radius R on the average SER of multi-user massive MIMO communication systems with irregular antenna arrays is evaluated in Fig. 7.

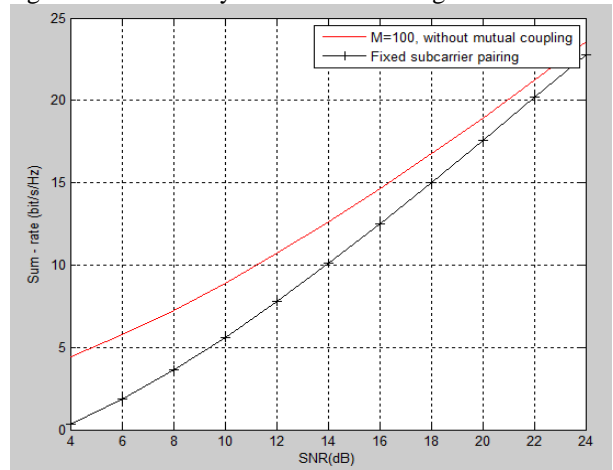


Fig6. Impact of the UT SNR and the number of BS antennas on the achievable sum rate of multi-user massive MIMO communication systems with and without mutual coupling.

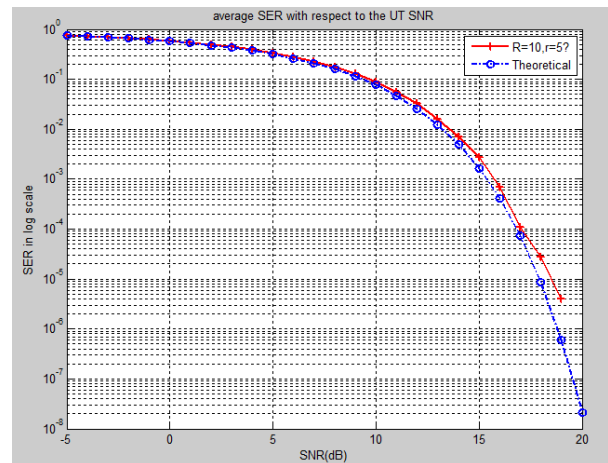


Fig7. The average SER with respect to the UT SNR, the number of BS antennas and the circle radius of the massive MIMO communication system with irregular antenna arrays. Both cases with limited and infinite numbers of antennas are illustrated.

The solid and dashed lines corresponds to the SER with limited number of antennas under different circle radii. And the square points correspond to the asymptotic results obtained in . When the number of BS antennas and the circle radius are fixed, the average SER decreases with the increase of the UT SNR. When the UT SNR and the circle radius are fixed, the average SER decreases with the increase of the number of BS antennas. When the UT SNR and the number of BS antennas are fixed, the average SER decreases with the increase of the circle radius. The average outage probability with respect to the UT SNR, the number of BS antennas and the circle radius is analyzed in Fig. 8. Without loss of generality, the SNR threshold is

configured as $SNR_{th} = -3$ dB. When the number of BS antennas and the circle radius are fixed, the average outage probability of massive MIMO communication systems with irregular antenna arrays decreases with the increase of the UT SNR.

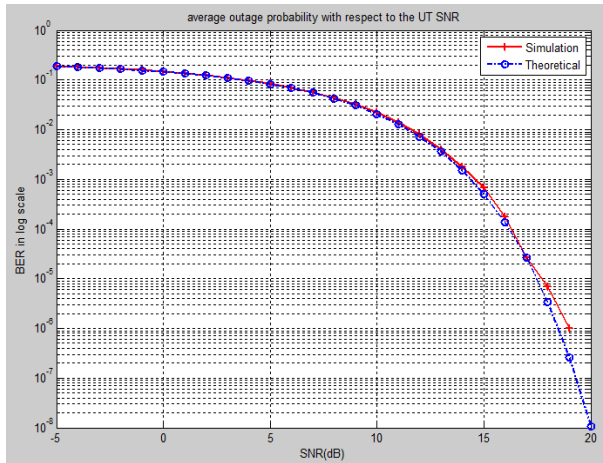


Fig8. The average outage probability with respect to the UT SNR, the number of BS antennas and the circle radius of the massive MIMO communication system with irregular antenna arrays.

When the UT SNR and the circle radius are fixed, the average outage probability of massive MIMO communication systems with irregular antenna arrays decreases with the increase of the number of BS antennas. When the UT SNR and the number of BS antennas are fixed, the average outage probability of massive MIMO communication systems with irregular antenna arrays decreases with the increase of the circle radius.

VI. CONCLUSION

In this paper, multi-user massive MIMO communication systems through irregular antenna arrays and mutual coupling effects have been investigated and a new update technique utilizing Householder conversion mutually with the LMS algorithm has been proposed for the adaptive DFGSC to compact with the nonstationary signal atmosphere. In real antenna deployment scenarios, antenna spatial distances of massive MIMO antenna arrays are usually irregular. Considering engineering requirements from real scenarios, the effect of the mutual coupling on the irregular antenna array is firstly analyzed by the channel correlation model and ergodic received gain. Furthermore, the lower bound of the ergodic achievable rate, the average SER and the average outage probability of multi-user massive MIMO communication systems with irregular antenna arrays are proposed. Numerical results indicate that there exists a maximum for the achievable rate considering different numbers of antennas for massive MIMO communication systems. Evaluated with the normal antenna array, the irregular antenna array has donated to improve the attainable rate when the number of antennas is

superior than or equal to a specific threshold. Our results provide some guidelines for the massive MIMO antenna deployment in real settings. For the future study, we will try to investigate multi-cell multi-user massive MIMO communication systems with irregular antenna arrays.

REFERENCES

- [1] X. Ge, S. Tu, G. Mao, C.-X. Wang, and T. Han, "5G ultra-dense cellular networks," *IEEE Wireless Commun.*, vol. 23, no. 1, pp. 72–79, Feb. 2016.
- [2] X. Ge, H. Cheng, M. Guizani, and T. Han, "5G wireless backhaul networks: Challenges and research advances," *IEEE Netw.*, vol. 28, no. 6, pp. 6–11, Nov. 2014.
- [3] M. Chen, Y. Zhang, Y. Li, S. Mao, and V. C. M. Leung, "EMC: Emotionaware mobile cloud computing in 5G," *IEEE Netw.*, vol. 29, no. 2, pp. 32–38, Mar./Apr. 2015.
- [4] A. Pitarokoilis, S. K. Mohammed, and E. G. Larsson, "On the optimality of single-carrier transmission in large-scale antenna systems," *IEEE Wireless Commun. Lett.*, vol. 1, no. 4, pp. 276–279, Aug. 2012.
- [5] Z. Xu, S. Sfar, and R. S. Blum, "Receive antenna selection for closely spaced antennas with mutual coupling," *IEEE Trans. Wireless Commun.*, vol. 9, no. 2, pp. 652–661, Feb. 2010.
- [6] T. Svantesson and A. Ranheim, "Mutual coupling effects on the capacity of multielement antenna systems," in *Proc. IEEE ICASSP*, May 2001, pp. 2485–2488.
- [7] F. Boccardi, R. W. Heath, A. Lozano, T. L. Marzetta, and P. Popovski, "Five disruptive technology directions for 5G," *IEEE Commun. Mag.*, vol. 52, no. 2, pp. 74–80, Feb. 2014.
- [8] C. A. Balanis, *Antenna Theory: Analysis and Design*. New York, NY, USA: Wiley, 2012.
- [9] J. Andersen and H. Rasmussen, "Decoupling and descattering networks for antennas," *IEEE Trans. Antennas Propag.*, vol. AP-24, no. 6, pp. 841–846, Nov. 1976.
- [10] I. J. Gupta and A. A. Ksienski, "Effect of mutual coupling on the performance of adaptive arrays," *IEEE Trans. Antennas Propag.*, vol. AP-31, no. 5, pp. 785–791, Sep. 1983.
- [11] P.-S. Kildal and K. Rosengren, "Correlation and capacity of MIMO systems and mutual coupling, radiation efficiency, and diversity gain of their antennas: Simulations and measurements in a reverberation chamber," *IEEE Commun. Mag.*, vol. 42, no. 12, pp. 104–112, Dec. 2004.
- [12] R. Janaswamy, "Effect of element mutual coupling on the capacity of fixed length linear arrays," *IEEE Antennas Wireless Propag. Lett.*, vol. 1, no. 1, pp. 157–160, Jan. 2002.
- [13] B. Clerckx, C. Craeye, D. Vanhoenacker-Janvier, and C. Oestges, "Impact of antenna coupling on 2×2 MIMO communications," *IEEE Trans. Veh. Technol.*, vol. 56, no. 3, pp. 1009–1018, May 2007.
- [14] J. W. Wallace and M. A. Jensen, "Mutual coupling in MIMO wireless systems: A rigorous network theory analysis," *IEEE Trans. Wireless Commun.*, vol. 3, no. 4, pp. 1317–1325, Jul. 2004.
- [15] T. L. Marzetta, "Noncooperative cellular wireless with unlimited numbers of base station antennas," *IEEE Trans. Wireless Commun.*, vol. 9, no. 11, pp. 3590–3600, Nov. 2010.
- [16] H. Q. Ngo, E. G. Larsson, and T. L. Marzetta, "Energy and spectral efficiency of very large multiuser MIMO systems," *IEEE Trans. Commun.*, vol. 61, no. 4, pp. 1436–1449, Apr. 2013.
- [17] M. Chen, Y. Hao, Y. Li, C. Lai, and D. Wu, "On the computation offloading at ad hoc cloudlet: Architecture and service models," *IEEE Commun.*, vol. 53, no. 6, pp. 18–24, Jun. 2015.

- [18] S. K. Mohammed, "Impact of transceiver power consumption on the energy efficiency of zero-forcing detector in massive MIMO systems," *IEEE Trans. Commun.*, vol. 62, no. 11, pp. 3874–3890, Nov. 2014.
- [19] J. Chen and V. K. N. Lau, "Two-tier precoding for FDD multi-cell massive MIMO time-varying interference networks," *IEEE J. Sel. Areas Commun.*, vol. 32, no. 6, pp. 1230–1238, Jun. 2014.
- [20] A. J. Duly, T. Kim, D. J. Love, and J. V. Krogmeier, "Closed-loop beam alignment for massive MIMO channel estimation," *IEEE Commun. Lett.*, vol. 18, no. 8, pp. 1439–1442, Aug. 2014.
pp. 2862–2871, Aug. 2011